The maximum-entropy inference of solutions to PDEs

1998 J. Phys. A: Math. Gen. 31 757

(http://iopscience.iop.org/0305-4470/31/2/030)

J. Phys. A: Math. Gen. **31** (1998) 757–765. Printed in the UK PII: S0305-4470(98)85494-2

The maximum-entropy inference of solutions to PDEs

E D Malaza†

Applied Mathematics, University of the North, PO Sovenga 0727, Republic of South Africa

Received 1 July 1997, in final form 2 September 1997

Abstract. We use the maximum-entropy variational technique to infer solutions to second-order partial differential equations. We restrict ourselves to problems with Dirichlet boundary conditions. First, we construct a basis of moment functions in terms of which we set up the constraints for a maximum entropy inversion for the inference of solutions to elliptic equations. Then we extend the scheme to the inference of time dependence in evolution equations. This extension is done by solving a small system of first-order initial-value differential equations for the moments of the solution vector.

1. Introduction

The application of variational techniques to the approximation of solutions to boundary-value problems (BVPs) is well established [1]. In these techniques, the BVP is transformed into a variational boundary-value problem (VBVP) which has certain computational advantages over the original BVP. The important advantage, under certain conditions, is that the VBVP is equivalent to a minimization problem that can be solved by a suitable choice of a small number of basis functions.

The maximum-entropy method (MaxEnt) [2–4], based on information theory [5–7], is a powerful inference technique that has been applied in many areas [8–10]. The recent MaxEnt scheme of Baker-Jarvis and his collaborators [11–13] has formulated BVPs in terms of VBVPs expressed as a set of moment equations in a one-dimensional grid. The solution vector is found as averages over a normalized probability distribution determined by maximizing an entropy or information measure with constraints provided by the VBVP and a condition of a fixed norm on the solution vector. The advantage of this framework is that the solution is expressed by a simple product of matrices independent of the Lagrange multipliers. The outstanding problem in the Baker-Jarvis scheme was the construction of basis moment functions such that the VBVP equation provides, for a small set of basis functions, optimum information for the maximum entropy inversion. An efficient basis for one-dimensional linear BVPs has just been developed [14].

The main aim of this work is the development of a MaxEnt method for the inference of solution to second-order partial differential equations (PDEs). This involves the determination of an efficient basis or moment functions in two dimensions. In addition, such a basis is useful in the inference of solutions to evolution equations. An application to simple time-dependent problems involving one space dimension has recently been done, yielding very good approximation to analytical solutions [15]. This inference of time dependence is

† E-mail address: malaza_ed@unin1.unorth.ac.za

achieved by following the time evolution of a few moments of the solution function. This approach is consistent with other MaxEnt methods for this class of problems [16–21].

The work is organized as follows. In section 2 we derive the VBVP for elliptic PDEs defined over a rectangular domain in $\mathbb{R}^2$. In section 3 we propose a two-dimensional moment basis that is a generalization of the one-dimensional one developed in [14]. In section 4.1 we give expressions for the matrices that occur in a MaxEnt minimum-norm solution to BVPs described by elliptic PDEs as well as numerical examples. Section 4.2 gives the extension to time-dependent problems, i.e. an extension to hyperbolic and parabolic equations. Finally, conclusions are drawn in section 5.

2. MaxEnt variational boundary-value problem

We consider the BVPs of the form

$$\begin{aligned} Lu(\boldsymbol{x}) &= f(\boldsymbol{x}) \qquad \boldsymbol{x} \in \boldsymbol{\Omega} \subset \mathbb{R}^2 \\ u &= g \qquad \text{on } \Gamma \end{aligned} \tag{2.1}$$

where the function g specifies the value of the unknown function u on the boundary Γ of a rectangular solution domain Ω in which the second-order operator L, of the form

$$L = a_{20}(\boldsymbol{x})\frac{\partial^2}{\partial x^2} + a_{11}(\boldsymbol{x})\frac{\partial^2}{\partial x \partial y} + a_{02}(\boldsymbol{x})\frac{\partial^2}{\partial y^2} + a_{10}(\boldsymbol{x})\frac{\partial}{\partial x} + a_{01}(\boldsymbol{x})\frac{\partial}{\partial y} + a_{00}(\boldsymbol{x}) \tag{2.2}$$

is elliptic. Let $\boldsymbol{\xi} \in \mathbb{R}^2$ and $\alpha = (\alpha_1, \alpha_2) \in Z_2^+$, then the operator A is elliptic at the point $\boldsymbol{x}_0 \in \Omega$ if

$$\sum_{|\alpha|=2} a_\alpha(\boldsymbol{x}_0)\boldsymbol{\xi}^\alpha \neq 0 \tag{2.3}$$

where $\boldsymbol{\xi}^\alpha = \xi^{\alpha_1}\xi^{\alpha_2}$.

We transform the BVP (2.1) to a moment problem by multiplying both sides by an appropriate basis of functions $\{v_{m_1m_2}(\boldsymbol{x})\}$, where $m_1 = 1, 2, \ldots, M_1$ and $m_2 = 1, 2, \ldots, M_2$, and integrating over the domain $\boldsymbol{\Omega}$. For the left-hand side, repeated integration by parts is used to obtain an expression of the form

$$\int_\Omega v_{m_1m_2}(\boldsymbol{x})Lu(\boldsymbol{x})\,\mathrm{d}\Omega = \int_\Gamma F(v_{m_1m_2}, u)\,\mathrm{d}s + \int_\Omega u(\boldsymbol{x})L^\dagger v_{m_1m_2}(\boldsymbol{x})\,\mathrm{d}\Omega \tag{2.4}$$

where $L^\dagger$ is the adjoint operator corresponding to L. Our construction of the basis functions $\{v_{m_1m_2}(\boldsymbol{x})\}$ is such that $v_{m_1m_2}(\boldsymbol{x})$ vanishes on the boundary Γ.

Transposing the boundary term in (2.4) to the transformed right-hand side of (2.1), we get the following variational or moment problem corresponding to (2.1): find the solution $u(\boldsymbol{x})$ which satisfies the equation

$$R(v_{m_1m_2}) = \int_\Omega G_{m_1m_2}(\boldsymbol{x})u(\boldsymbol{x})\,\mathrm{d}\Omega \tag{2.5}$$

for the basis $\{v_{m_1m_2}(\boldsymbol{x})\}$, where

$$G_{m_1m_2}(\boldsymbol{x}) = L^\dagger v_{m_1m_2}(\boldsymbol{x}) \tag{2.6}$$

and

$$R(v_{m_1m_2}) = \int_\Omega v_{m_1m_2}(\boldsymbol{x})f(\boldsymbol{x})\,\mathrm{d}\Omega - \int_\Gamma F(v_{m_1m_2}, u)\,\mathrm{d}s. \tag{2.7}$$

Now, we discretize the rectangular domain Ω. Let h_1 and h_2 be the space steps in the x_1 and x_2 directions, respectively, and denote $u(\boldsymbol{x})$ by $u(x_{1i}, x_{2j})$, where $i = 0, 1, \ldots, n_1$

and $j = 0, 1, \ldots, n_2$, at the grid points. Then the integral on the right-hand side of (2.5) is replaced by the sum over the internal nodal points and the boundary terms are absorbed into the expression for $R(v_m)$. This results in the following replacement:

$$\int_\Omega G_{m_1 m_2}(\boldsymbol{x}) u(\boldsymbol{x})\, \mathrm{d}\Omega \to \sum_{i=1}^{n_1-1} \sum_{j=1}^{n_2-1} G_{m_1 m_2}(x_{1i}, x_{2j}) u(x_{1i}, x_{2j}).$$

It is convenient to transform the two-dimensional (i, j) grid into a one-dimensional one by the transformation

$$\begin{aligned} &(i, j) \to \gamma = i + (n_1 - 1)(j - 1) \\ &\gamma = 1, 2, \ldots, nt \qquad nt = (n1 - 1)(n2 - 1). \end{aligned} \tag{2.8}$$

For a given γ, the inverse transformation is

$$\begin{aligned} x_1(\gamma) &= a + h_1(\mathrm{Mod}(\gamma - 1, n_1 - 1) + 1) \\ x_2(\gamma) &= c + h_2(I((\gamma - 1)/(n_1 - 1)) + 1) \end{aligned}$$

where $I(m/n)$ denotes the greatest integer less than or equal to m divided by n, and $\mathrm{Mod}(m, n)$ denotes m modulus n. The moment indices m_1 and m_2 are similarly collapsed into one index $m = 1, 2, \ldots, M$, where $M = M_1 M_2$, by the transformation

$$\begin{aligned} &(m_1, m_2) \to m = m_1 + (M_1 - 1)(m_2 - 1) \\ &m = 1, 2, \ldots, M \qquad M = M_1 \times M_2. \end{aligned}$$

Then the discretized version of the inverse-moment problem (2.5) is of the form

$$R(v_m) = \sum_{\gamma=1}^{nt} G_{m\gamma} u_\gamma. \tag{2.9}$$

We now define the MaxEnt probability distribution globally over the entire one-dimensional grid, labelled by the index γ, and denoted by $P(\boldsymbol{u})$, where the vector $\boldsymbol{u}$ is over the entire grid $\boldsymbol{u} = (u_1, u_2, \ldots, u_{nt})$. We determine such a probability distribution, consistent with the information content (2.9), by maximizing the Shannon entropy

$$S = -\int_{-\infty}^{\infty} P(\boldsymbol{u}) \log P(\boldsymbol{u})\, \mathrm{d}\boldsymbol{u}. \tag{2.10}$$

This MaxEnt variational method has a well known analytical solution [22–24] and the minimum-norm solution that maximizes S subject to a normalized probability distribution $P(\boldsymbol{u})$, the information (2.9) and a fixed norm for the solution vector $\boldsymbol{u}$ is given by [11–13]

$$\boldsymbol{u} = \mathbf{G}^t(\mathbf{G}\mathbf{G}^t)^{-1}\mathbf{R} \tag{2.11}$$

where the matrices $\mathbf{G}$ and $\mathbf{R}$ are determined by equation (2.9), their dimensions being $M \times nt$ and $M \times 1$ respectively.

3. Construction of the moment basis

An efficient moment basis for the solution of one-dimensional BVPs using MaxEnt was constructed in [14]. For example, for a BVP in the region $\Omega = [a, b]$ the basis is

$$v_m^{(1)} = (x - a)^{1+I(m/2)}(x - b)^{1+I((m-1)/2)} \qquad m = 1, 2, \ldots, M. \tag{3.1}$$

For the two-dimensional case $\Omega = [a, b] \times [c, d]$ the moment basis can be constructed in either direction according to (3.1) with moment indices $m_1 = 1, 2, \ldots, M_1$ and $m_2 = 1, 2, \ldots, M_2$. The two indices (m_1, m_2) are then transformed into one index m

by a transformation similar to (2.8). The resulting moment function basis constructed this way can be written in the form

$$v_m(x_1, x_2) = \left(\frac{x1 - b}{b - a}\right)^{p_1(m)} \left(\frac{x1 - a}{b - a}\right)^{p_2(m)} \left(\frac{x2 - d}{d - c}\right)^{p_3(m)} \left(\frac{x2 - c}{d - c}\right)^{p_4(m)}$$
$$m = 1, 2, \ldots, M \tag{3.2}$$

where

$$\begin{aligned} p_1(m) &= I((\mathrm{Mod}(m - 1, M_1) + 1)/2) + 1 \\ p_2(m) &= I(\mathrm{Mod}(m - 1, M_1)/2) + 1 \\ p_3(m) &= I((I((m - 1)/M_1) + 1)/2) + 1 \\ p_4(m) &= I((I((m - 1)/M_1))/2) + 1. \end{aligned} \tag{3.3}$$

4. Applications

4.1. Time-independent partial differential equations

We consider the strongly elliptic problems of the form

$$\begin{aligned} &Lu(\boldsymbol{x}) = \nabla^2 u(\boldsymbol{x}) = \left(\frac{\partial^2}{\partial x_1^2} + \frac{\partial^2}{\partial x_2^2}\right) u(\boldsymbol{x}) = f(\boldsymbol{x}) \\ &\Omega = [a, b] \times [c, d] \\ &u(a, x_2) = g_1(x_2) \qquad u(b, x_2) = g_2(x_2) \qquad x_2 \in [c, d] \\ &u(x_1, c) = r_1(x_1) \qquad u(x_1, d) = r_2(x_1) \qquad x_1 \in [a, b]. \end{aligned} \tag{4.1}$$

For these problems, the solution is of the form (2.11) with the matrix **G** given by

$$G_{m\gamma} = h_1 h_2 [v_{m,xx}(x_1(\gamma), x_2(\gamma)) + v_{m,yy}(x_1(\gamma), x_2(\gamma))] \tag{4.2}$$

where $v_{m,xx}$ and $v_{m,yy}$ denote the second derivatives of v_m with respect to x and y respectively, and the components of the vector $\boldsymbol{R}$ given by

$$\begin{aligned} R_m = &\int_\Omega v_m(x_1, x_2) f(x_1, x_2)\, \mathrm{d}x_1\, \mathrm{d}x_2 \\ &+ \int_a^b [r_2(x_1)\{v_{m,y}(x_1, d) - \tfrac{1}{4} h_2(v_{m,xx}(x_1, d) + v_{m,yy}(x_1, d))\} \\ &- r_1(x_1)\{v_{m,y}(x_1, c) + \tfrac{1}{4} h_2(v_{m,xx}(x_1, c) + v_{m,yy}(x_1, c))\}]\, \mathrm{d}x_1 \\ &+ \int_c^d [g_2(x_2)\{v_{m,x}(b, x_2) - \tfrac{1}{4} h_1(v_{m,xx}(b, x_2) + v_{m,yy}(b, x_2))\} \\ &- g_1(x_2)\{v_{m,y}(a, x_2) + \tfrac{1}{4} h_1(v_{m,xx}(a, x_2) + v_{m,yy}(a, x_2))\}]\, \mathrm{d}x_2 \\ &- \frac{h_1 h_2}{4} \sum_{i=1}^{n_1 - 1} [r_2(x_i)(v_{m,xx}(x_i, d) + v_{m,yy}(x_i, d)) \\ &+ r_1(x_i)(v_{m,xx}(x_{1i}, c) + v_{m,yy}(x_{1i}, c))] \\ &- \frac{h_1 h_2}{4} \sum_{j=1}^{n_2 - 1} [g_2(x_{2j}) v_{m,xx}(b, x_{2j}) + v_{m,yy}(b, x_{2j}) \\ &+ g_1(x_{2j}) v_{m,xx}(a, x_{2j}) + v_{m,yy}(a, x_{2j})]. \end{aligned} \tag{4.3}$$

Using the basis (3.2), we obtain the matrix **G** in the form

$$G_{m\gamma} = v_m(x_1(\gamma), x_2(\gamma))\left[\frac{Z(p_3(m), p_4(m), x_2(\gamma)-c, x_2(\gamma)-d)}{(x_2(\gamma)-c)(x_2(\gamma)-d)} + \frac{Z(p_1(m), p_2(m), x_1(\gamma)-a, x_1(\gamma)-b)}{(x_1(\gamma)-a)(x_1(\gamma)-b)}\right] \tag{4.4}$$

where

$$Z(m,n,a,b) \equiv m(m-1)b^2 + 2mnab + n(n-1)a^2 \tag{4.5}$$

and the components of the vector $\boldsymbol{R}$ in the form

$$\begin{aligned} R_m = {} & \frac{1}{h_1h_2}\int_a^b\int_c^d v_m(x_1,x_2) f(x_1,x_2)\,\mathrm{d}x_1\,\mathrm{d}x_2 \\ & + \frac{1}{h_1h_2}\int_a^b (x_1-a)^{p1(m)}(x_1-b)^{p2(m)}[sx(p_4(m), p_3(m), d-c, x_1) \\ & -\tfrac{1}{4}\{T(p_4(m), p_3(m), d-c)r_2(x_1) + T(p_3(m), p_4(m), c-d)r_1(x_1)\}h_2]\,\mathrm{d}x_1 \\ & + \frac{1}{h_1h_2}\int_c^d (x_2-c)^{p3(m)}(x_2-d)^{p4(m)}[sy(p_2(m), p_1(m), b-a, x_2) \\ & -\tfrac{1}{4}\{T(p_2(m), p_1(m), b-a)g_2(x_2) + T(p_1(m), p_2(m), a-b)g_1(x_2)\}h_1]\,\mathrm{d}x_2 \\ & -\tfrac{1}{4}\left[\sum_{i=1}^{n1-1}(x_{1i}-a)^{p_1(m)}(x_{1i}-b)^{p(m)}\{r_2(x_{1i})T(p_4(m), p_3(m), d-c)\right. \\ & + r_1(x_{1i})T(p_3(m), p_4(m), c-d)\} \\ & + \sum_{j=1}^{n2-1}(x_{2j}-c)^{p_3(m)}(x_{2j}-d)^{p_4(m)}\{g_2(x_{2j})T(p_2(m), p_1(m), b-a) \\ & \left. + g_1(x_{2j})T(p_1(m), p_2(m), a-b)\}\right] \end{aligned} \tag{4.6}$$

where

$$\begin{aligned} & T(m,n,a) \equiv m(m-1)a^n\delta_{m,2} + 2mna^{n-2}\delta_{m,1} \\ & sx(m,n,a,x) \equiv ma^n r_2(x)\delta_{m,1} - n(-a)^m r_1(x)\delta_{n,1} \\ & sy(m,n,a,y) \equiv ma^n g_2(y)\delta_{m,1} - n(-a)^m g_1(y)\delta_{n,1}. \end{aligned} \tag{4.7}$$

4.1.1. Numerical example. Now we present numerical examples in the solution of problems of the form (4.1) using the minimum-norm scheme (2.11) with the matrices given by (4.4) and (4.6).

As a first example we solve (4.1) with

$$\begin{aligned} & f(\boldsymbol{x}) = -2 \qquad \Omega = [0,1]\times[0,1] \\ & g_1(x_2) = 0 \qquad g_2(x_2) = \sinh(\pi)\sin(\pi y) \\ & h_1(x_1) = h_2(x1) = x(1-x). \end{aligned} \tag{4.8}$$

Figure 1 shows the relative error of the MaxEnt inference, using $M_1 = M_2 = 8$, with reference to the exact solution $u(\boldsymbol{x}) = \sinh(\pi x)\sin(\pi y)$ for a grid of size $n_1 = n_2 = 100$. The errors are very small except near the $x_2 = 0$ boundary where their absolute value is around 0.03. Hence the percentage error in the MaxEnt inference is generally very small and is largest at about 3% near the $x_2 = 0$ boundary.

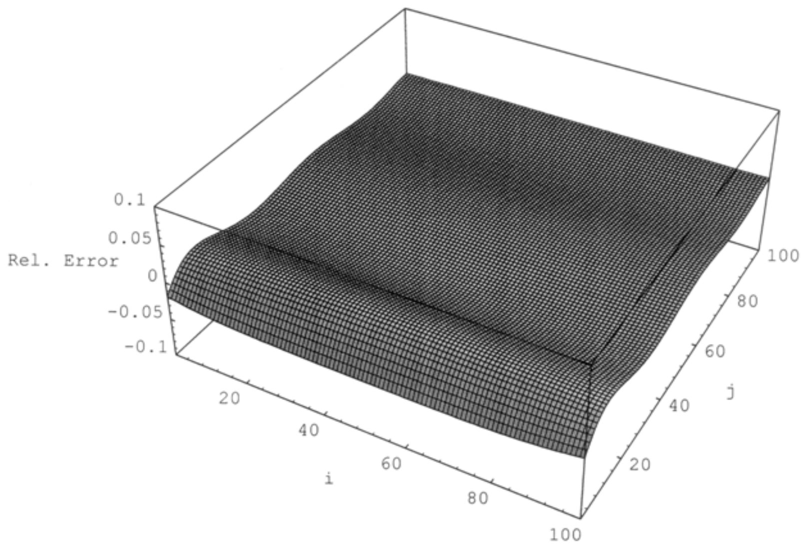

Figure 1. Relative error of MaxEnt inference, using $M_1 = M_2 = 8$, with reference to the exact solution $u(\boldsymbol{x}) = \sinh(\pi x)\sin(\pi y)$ for a grid of size $n_1 = n_2 = 100$ for the problem (4.8).

As a further example we solve (4.1) with

$$\begin{aligned} &f(\boldsymbol{x}) = (x_1^2 + x_2^2)\mathrm{e}^{x_1 x_2} \qquad \Omega = [0, 2] \times [0, 1] \\ &g_1(x_2) = 1 \qquad g_2(x_2) = \mathrm{e}^{2x_2} \\ &h_1(x_1) = 1 \qquad h_2(x1) = \mathrm{e}^{x_1}. \end{aligned} \tag{4.9}$$

We show the relative error of the MaxEnt inference, using $M_1 = M_2 = 9$, with reference to the exact solution $u(\boldsymbol{x}) = \mathrm{e}^{x_1 x_2}$ for a grid of size $n_1 = n_2 = 100$ in figure 2. For this example, the errors are extremely small with the largest being about 0.01. This region of appreciable area is a very small subset of the grid and the inference can hopefully be improved by enlarging the basis size M.

4.2. Evolution equations

The MaxEnt inference method developed above is quite useful in the inference of solutions to evolution equations. The moment basis (3.2) is used to sum the space dependence so that the PDE is transformed into a small system of ordinary differential equations in the moments

$$A_m(t) = \int_\Omega v_m(\boldsymbol{x}) u(\boldsymbol{x}, t)\, \mathrm{d}\Omega \qquad m = 1, 2, \ldots M. \tag{4.10}$$

We show how the MaxEnt minimum-norm scheme (2.11) closes, in an approximate way, the equations of motion of $A_m(t)$, thereby providing the inference of the solution $u(\boldsymbol{x}, t)$, through the following example of heat flow in a two-dimensional domain.

We seek an approximate numerical solution to the problem

$$\begin{aligned} &u_t = u_{xx} + u_{yy} \qquad 0 < x, y, < 1 \qquad t > 0 \\ &u(0, y, t) = u(1, y, t) = 0 \qquad 0 < y < 1 \qquad t > 0 \\ &u(x, 0, t) = u(x, 1, t) = 0 \qquad 0 < x < 1 \qquad t > 0 \\ &u(x, y, 0) = 100 \sin \pi x \sin \pi y \qquad 0 < x, y, < 1. \end{aligned} \tag{4.11}$$

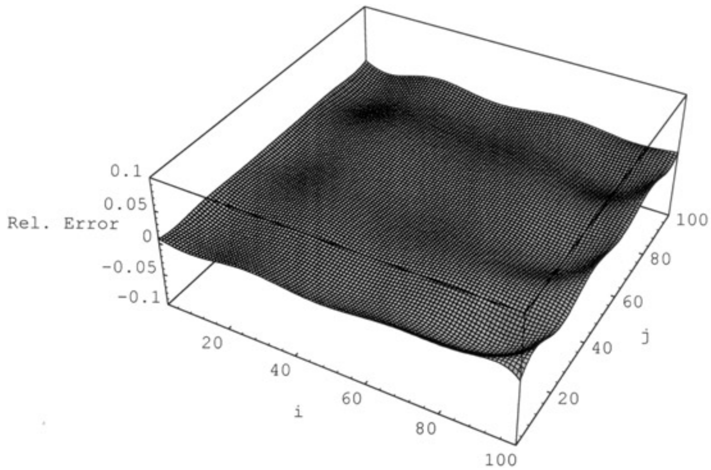

Figure 2. Relative error of MaxEnt inference, using $M_1 = M_2 = 9$, with reference to the exact solution $u(\boldsymbol{x}) = \mathrm{e}^{x_1 x_2}$ for a grid of size $n_1 = n_2 = 100$ for the problem (4.9).

Taking the moments of the PDE in (4.11) with the basis $\{v_m(\boldsymbol{x})\}$, we obtain the following equations

$$A_m(t) = \int_\Omega v_m(\boldsymbol{x}) u(\boldsymbol{x}, t)\, \mathrm{d}\Omega \tag{4.12}$$

$$\frac{\mathrm{d}}{\mathrm{d}t} A_m(t) = \int_\Omega u(\boldsymbol{x}, t)\{\nabla^2 v_m(\boldsymbol{x})\}\, \mathrm{d}\Omega. \tag{4.13}$$

Eliminating the minimum-norm solution vector $u(\boldsymbol{x}, t)$ between the equations (4.12) and (4.13) we obtain the evolution equation of the moment vector in the form

$$\begin{aligned} &\frac{\mathrm{d}}{\mathrm{d}t}\boldsymbol{A}(t) = \mathbf{G}\tilde{\mathbf{G}}(\tilde{\mathbf{G}}\tilde{\mathbf{G}}^t)^{-1} \\ &\boldsymbol{A}(0) = \int_\Omega \boldsymbol{v}(\boldsymbol{x}) u(\boldsymbol{x}, 0)\, \mathrm{d}\Omega \qquad m = 1, 2, \ldots, M \end{aligned} \tag{4.14}$$

where $\boldsymbol{A}^t = (A_1, A_2, \ldots, A_M)$, and $\boldsymbol{v}^t(\boldsymbol{x}) = (v_1(\boldsymbol{x}), v_2(\boldsymbol{x}), \ldots, v_M(\boldsymbol{x}))$. The matrix $\mathbf{G}$ depends on the space operator ∇^2 and the boundary conditions of (4.11) and, calculated by the procedure of the previous sections, is given by

$$\begin{aligned} &\tilde{G}_{m\gamma} = h_1 h_2 v_m(x(\gamma), y(\gamma)) \\ &m = 1, 2, \ldots, M \qquad \text{and} \qquad \gamma = 1, 2, \ldots, nt. \end{aligned}$$

The solution vector $u(\boldsymbol{x}, t)$ on the grid is then inferred as

$$\boldsymbol{u}(t) = \tilde{\mathbf{G}}(\tilde{\mathbf{G}}\tilde{\mathbf{G}}^t)^{-1}\boldsymbol{A}(t) \tag{4.15}$$

where $\boldsymbol{A}(t)$ is the solution of the initial-value problem (4.14).

We show the relative error of the inferred (4.15) solution for the example (4.11), on a grid of size $n_1 = n_2 = 50$ with $M_1 = M_2 = 4$, in figure 3 with reference to the analytical solution $u = 100\mathrm{e}^{-2\pi^2 t} \sin \pi x \sin \pi y$ at $t = 0.03$. The relative error is extremely small at all points and is of order 10^{-3}.

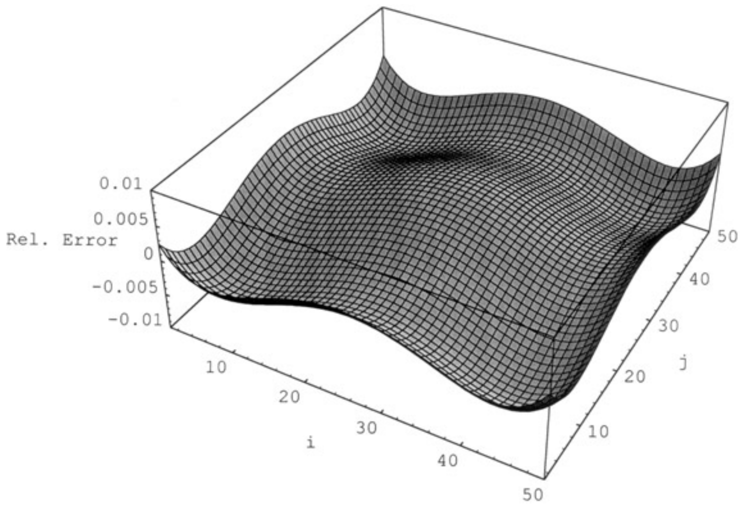

Figure 3. Relative error of MaxEnt inferred solution for the example (4.11), on a grid of size $n_1 = n_2 = 50$ with $M_1 = M_2 = 4$, with reference to the analytical solution $u = 100\mathrm{e}^{-2\pi^2 t} \sin \pi x \sin \pi y$ at $t = 0.03$.

5. Conclusions

We have derived a numerical procedure based on the MaxEnt minimum-norm method for the inference of solution to BVPs described by second-order PDEs. We have shown that this procedure gives a good approximation to the exact solution with relatively little information for a particular basis of moment functions. Although only problems with Dirichlet boundary conditions have been considered, it should be possible to extend this procedure to other forms of boundary conditions, possibly with a minor modification of the basis functions. The basis suggested here is superior to a Fourier basis that is often used in variational techniques [1] and has been considered in the context of the MaxEnt minimum-norm method [11–14].

This method is simple in that the inferred solution vector is expressed as a product of matrices determined by only two matrices, $\mathbf{G}$ and $\mathbf{R}$. These two matrices depend only on the form of the differential operator and on the boundary conditions of the problem. They are independent of the Lagrange multipliers used in maximizing the entropy subject to the VBVP constraints. This simplicity of the method makes it a viable alternative to the well-established approximation methods, such as the method of finite differences. The speed of the numerical calculation depends on the sizes of the matrices $\mathbf{G}$ and $\mathbf{R}$, especially on the evaluation of the inverse $(\mathbf{GG}^t)^{-1}$ which is largely dependent on the conditioning of the matrix product $\mathbf{GG}^t$. Ill-conditioning on the matrix $\mathbf{GG}^t$ can result in significant errors in the MaxEnt inversion. A report, by the numerical package used, on the conditioning of this matrix may serve as a useful guide to the adequacy of the information provided for the inversion.

The method has the capability to solve a wider class of problems involving evolution equations with an open space domain, such as the general solution to N-dimensional Fokker–Planck equations, provided one can choose an appropriate moment basis. Also it promises to be a robust tool for solving general inverse problems involving differential operators, such as the inverse problem for the Maxwell equations.

References

[1] Reddy B D *Functional Analysis and Boundary-value Problems* (New York: Longman Scientific and Technical and Wiley)
[2] Jaynes E T 1957 *Phys. Rev.* **106** 620
[3] Jaynes E T 1957 *Phys. Rev.* **108** 171
[4] Jaynes E T 1963 *Statistical Mechanics* ed W K Ford (New York: Benjamin)
[5] Khinchin A I 1957 *Mathematical Foundations of Information Theory* (New York: Dover)
[6] Shannon C E 1948 *Bell Syst. Tech. J.* **27** 379
[7] Shannon C E 1948 *Bell Syst. Tech. J* **27** 623
[8] Gull S F and Skilling J 1984 *IEE Proc.* F **131** 646
[9] Ulrych T *et al* 1990 *Geophys. Prospect.* **38** 465
[10] Malaza E D *et al* 1991 *J. Phys. B: At. Mol. Opt. Phys.* **266** 169
[11] Baker-Jarvis J, Racine M and Alamedine J 1989 *J. Math. Phys.* **30** 1459
[12] Baker-Jarvis J 1989 *J. Math. Phys.* **30** 302
[13] Baker-Jarvis J, Racine M, Alamedine J and Schultz D 1989 *Numer. Meth. Part. Diff. Eqns* **5** 133
[14] Malaza E D and Solms F *Preprint* University of the North UNIN/AMATH 6/1996
[15] Malaza E D, Solms F, Miller H G and Plastino A *Phys. Lett.* A submitted
[16] Plastino A R and Plastino A 1996 *Physica* **232A** 458
[17] Hick P and Stevens G 1987 *Astron. Astrophys.* **172** 350
[18] Alhassid Y and Levine R 1977 *J. Chem. Phys.* **67** 4321
[19] Alhassid Y and Levine R 1978 *Phys. Rev.* A **18** 89
[20] Otero D, Plastino A, Proto A N and Zannoli G 1982 *Phys. Rev.* A **26** 1209
[21] Otero D, Plastino A, Proto A N and Zannoli G 1984 *Phys. Rev.* A **316** 323
[22] Katz A 1967 *Statistical Mechanics* (San Francisco, CA: Freeman)
[23] Hobson A 1992 *Concepts in Statistical Mechanics* (London: Gordon and Breach)
[24] Balian R 1992 *From Microphysics to Macrophysics* (Berlin: Springer)